CHEMMEDCHEM

DOI: 10.1002/cmdc.200800265

Natural-Product-Like Spiroketals and Fused Bicyclic Acetals as Potential Therapeutic Agents for B-Cell Chronic Lymphocytic Leukaemia

Lech-Gustav Milroy,[a] Giovanna Zinzalla,[a] François Loiseau,[a] Zizheng Qian,[a] Giuseppe Prencipe,[a] Chris Pepper,[b] Chris Fegan,[b] and Steven V. Ley*[a]

B-cell chronic lymphocytic leukaemia (CLL) is the most common form of leukaemia in the Western world for which no curative treatments are currently available. Purine nucleotide analogues and alkylating agents feature frequently in combination regimens to treat the malignant state, but their use has not led to any significant improvement in patient survival. Consequently, there still remains a need for alternative small-molecule chemotherapeutics. Natural products are an unparalleled source of drug leads, and an unending inspiration for the design of small-molecule libraries for drug discovery. The screening of focused libraries of natural-product-like spiroketal and fused bicyclic acetal small molecules against primary CLL cells has led to the identification of a small series of novel and potent cytotoxic agents towards primary CLL cells. The validation of the activity of these molecules is delineated through a series of synthesis and screening iterations, whereas preliminary mode of action studies positively indicate their ability to induce cell death via an apoptotic pathway with no evidence of necrosis to further support their potential as novel chemotherapeutic agents.

Introduction

B-cell chronic lymphocytic leukaemia (CLL) is a disease characterised by the clonal expansion of CD5+/CD19+ B-cells. It is the most common leukaemia in the Western world, responsible for 5,000 deaths annually in the United States alone.[1,2] The clinical course of CLL is heterogeneous: whereas some patients have normal age-adjusted survival, the median survival of those suffering with the advanced-stage disease is only 36 months and in spite of some advances in chemotherapy, CLL remains incurable.

Over the last four decades, chlorambucil (**1**) (shown) has been the mainstay of treatment for this condition. However, the complete response rates obtained with this agent are low (10%) and consequently it has made little impression on the natural pathology of the disease.[3] Purine analogues, particularly, fludarabine (**2**), are more effective against CLL, with a higher complete response rate than chlorambucil and other DNA-alkylating-based chemotherapies (20-40% versus 10%).[4–6] However, despite inducing a longer disease-free interval these agents have failed to prolong survival. The use of monoclonal antibodies such as rituximab and alemtuzumab has produced higher response rates in chemonaive patients,[7–9] and today, treatment of CLL has switched to purine analogue-based regimes in combination with alkylating agents and/or monoclonal antibodies. This multidrug approach has resulted in higher response rates and longer disease-free survival than historical monotherapies.[10–13] Indeed, immunochemotherapy is increasingly considered to be the new standard for treating patients with CLL. However, the best combination chemotherapy has not yet been identified. More recently, the sequence specific, p53-independent DNA cross-linking agent SJG-136 (**3**)[14] and Mdm2-inhibitor (±)-Nutlin-3 (**4**)[15] have emerged as potential alternative cytotoxic agents. At present, allogeneic hae-

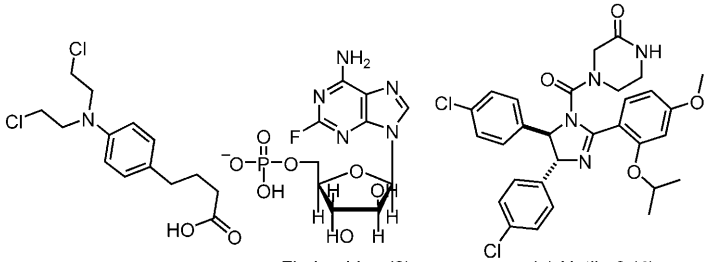

Chlorambucil (**1**) Fludarabine (**2**) (±)-Nutlin-3 (**4**)

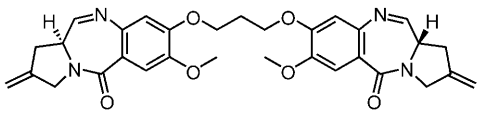

SJG-136 (**3**)

[a] Dr. L.-G. Milroy, Dr. G. Zinzalla, Dr. F. Loiseau, Z. Qian, G. Prencipe, Prof. Dr. S. V. Ley
Department of Chemistry, University of Cambridge, Lensfield Road, Cambridge, CB2 1EW (UK)
Fax: (+44) 122-333-6442
E-mail: svl1000@cam.ac.uk

[b] Dr. C. Pepper, Dr. C. Fegan
Department of Haematology, School of Medicine, Cardiff University, Heath Park, Cardiff, CF14 4XN (UK)

Supporting information for this article is available on the WWW under http://dx.doi.org/10.1002/cmdc.200800265.

matopoietic cell transplantation (HCT) is the only potentially curative therapy for CLL,[2,16] but due to the high treatment-related mortality and the advanced age of many patients, the procedure is not widely applicable. Therefore, there exists a critical need for both novel therapeutic agents and alternative approaches for the improved treatment of this disease.

Recently, we reported in two separate papers the design and synthesis of natural-product- and drug-like small molecules based on the spiroketal[17] and fused bicyclic acetal[18] molecular frameworks (shown). These two structures are found

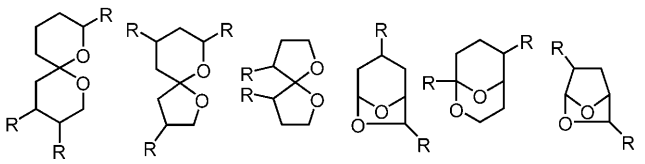

recurrently in natural products with impressive anticancer properties,[19] a few examples of which are also shown.[20–22] On these grounds and based on the fact that they would allow us to introduce a high degree of structural diversity for the preparation of compound libraries, we envisaged the potential use of these structures as scaffolds to identify new chemotherapeutic agents. Our preliminary studies into the effect of our compounds on cancer cell proliferation have given encouraging results, which we are currently investigating further. In particular, a cancer cell viability screen of a focused set of fused bicyclic acetals has shown some promising activity and, above all, selectivity across compounds **5**–**7** (Figure 1).[18]

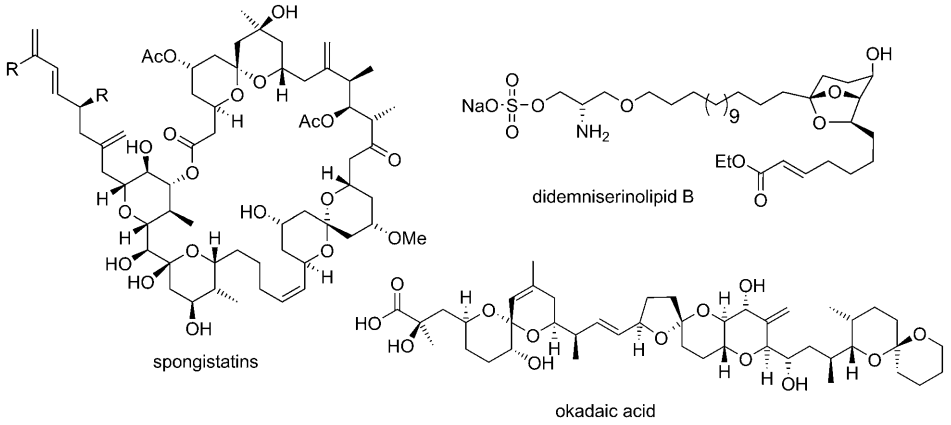

Herein we report the results from a separate biological study into the effects of our molecules against primary CLL cells. We describe the outcome of a first generation screen, highlight emerging structure–activity relationship (SAR) trends and combine these with our growing knowledge of the synthesis of these two classes of molecule to improve the potency of the series through the preparation of focused compound collections. Subsequent screening rounds were performed against CLL cells taken from different patients, each expressing different prognostic marker profiles. However, it should be noted that within each screening iteration, donor cells from a single patient were used to ensure that the potency of the compounds being tested could be directly compared. This work culminates in the identification and validation of a series of new inhibitors for the treatment of CLL that affect apoptosis via a classical drug-induced intrinsic pathway at submicromolar concentrations. These molecules have shown improved potency (mole per mole) when compared with fludarabine in the same screen.

Results and Discussion

Biological evaluation of the first generation of focused libraries

Twenty six structurally unique bicyclic acetals, fifteen spiroketals (Table 1, entries 1–15, compounds **8**–**22**)[17] and eleven fused bicylic acetals (Table 1, entries 16–26, compounds **23**–**33**)[18] were screened against primary CLL cells using flow cytometry to quantify their cytotoxic effects. This compound set found activity with LD_{50} values ranging from 0.8 to $>1000\ \mu M$.[23] Furthermore, a well-defined SAR was identified within both series that could be used to guide the preparation of a second generation of focused libraries.

For the spiroketal series (Table 1, entries 1–15) the most active compound was **16** (entry 9, $LD_{50} = 1.6\ \mu M \pm 0.4$). Aromatic substitution of the benzylic ether group (Scheme 1) led to a measurable increase in activity (compare **8** and **9**), whereas changes in stereochemistry at C6 and C10 (compare **9**–**11**, entries 2–4) produced a marked variation in potency, which was particularly interesting in view of the structural differences between the three compounds. The 1,3-dithianyl ring also

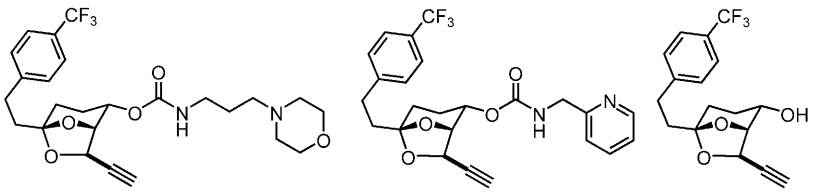

		5	**6**	**7**
MCF7	IC_{50} (μM)	9.3	9.0	>25.0
A549	IC_{50} (μM)	15.2	>25.0	>25.0

Figure 1. Preliminary biological results for simplified fused bicyclic acetal derivatives (**5**-**7**).

Table 1. First generation screening results

Entry	Structure	Cmpd no. (purity)[a]	LD_{50} [μM] (±S.D.)
1	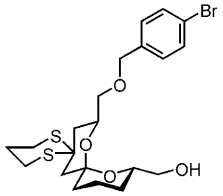	**8** (90-95)	4.8 (0.3)
2	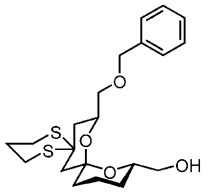	**9** (90)	>1000 (–)
3	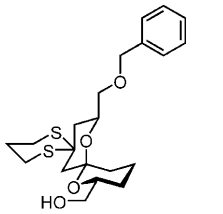	**10** (85-90)	3.7 (0.3)
4	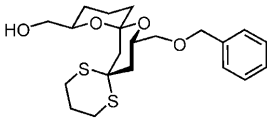	**11** (90)	20.0 (0.4)
5	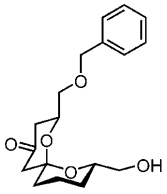	**12** (90-95)	>1000 (–)
6	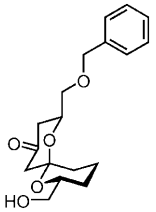	**13** (90-95)	>1000 (–)
7	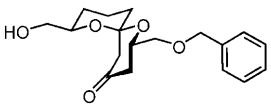	**14** (90)	45.2 (0.3)
8	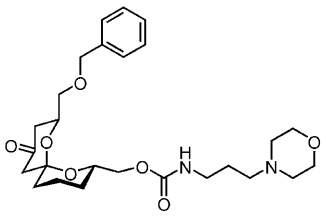	**15** (85-90)	29.4 (0.5)
9	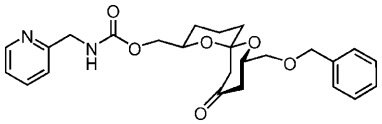	**16** (85)	1.6 (0.4)

Table 1. (Continued)

Entry	Structure	Cmpd no. (purity)[a]	LD_{50} [μM] (±S.D.)
10	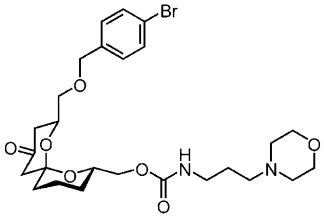	**17** (85-90)	17.1 (0.6)
11	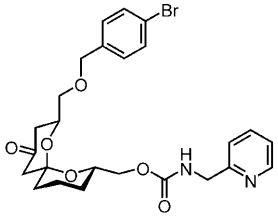	**18** (85-90)	38.2 (0.6)
12	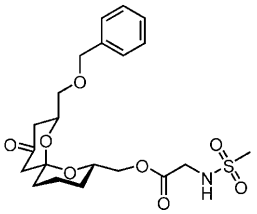	**19** (95)	>1000 (–)
13	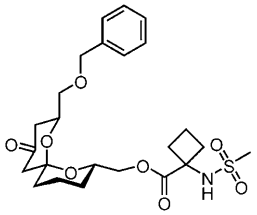	**20** (95)	>1000 (–)
14	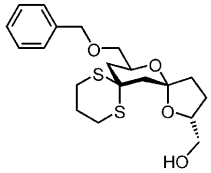	**21** (90)	>1000 (–)
15	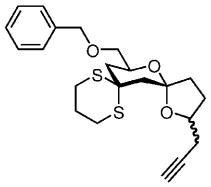	**22** (85)	7.9 (0.2)
16	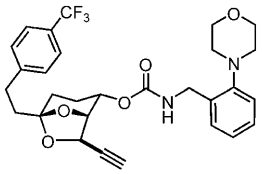	**23** (85)	31.0 (0.5)
17	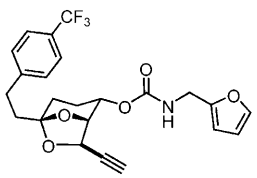	**24** (95)	>1000 (–)

Table 1. (Continued)

Entry	Structure	Cmpd no. (purity)[a]	LD_{50} [μM] (±S.D.)
18	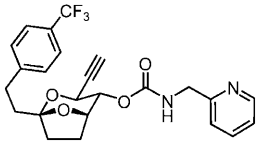	**25** (95)	>1000 (–)
19	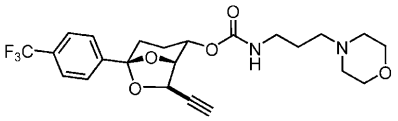	**26** (95)	5.2 (0.5)
20	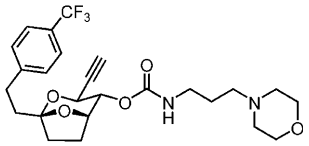	**27** (95)	3.4 (0.6)
21	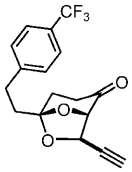	**28** (90)	39.3 (0.4)
22	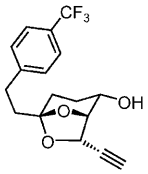	**29** (95)	0.8 (0.5)
23	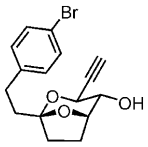	**30** (90)	>1000 (–)
24	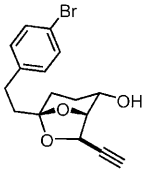	**31** (95)	44.4 (0.2)
25	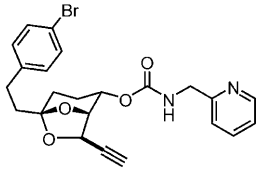	**32** (95)	>1000 (–)
26	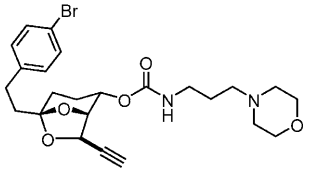	**33** (95)	1.6 (0.4)

[a] Compound purity determined spectroscopically using ^{1}H NMR and LC-MS.

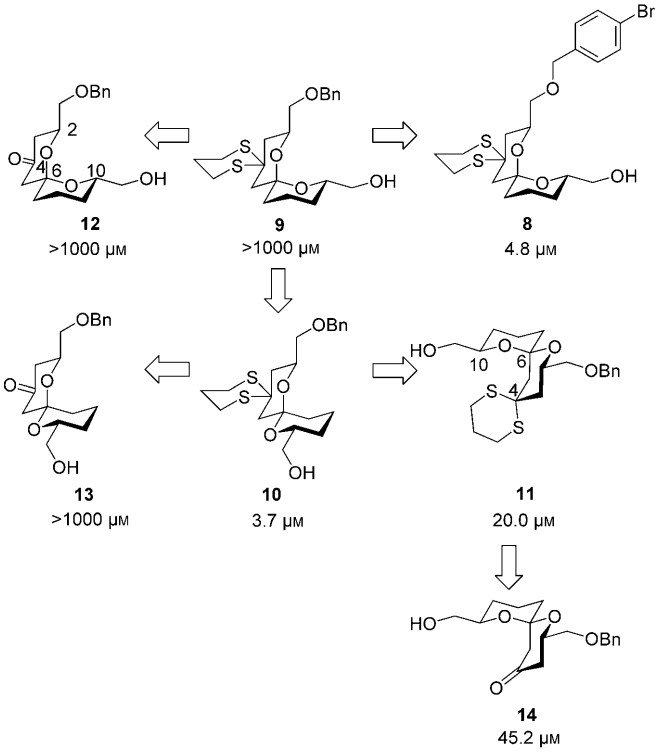

Scheme 1. Suggested spiroketal SAR: aromatic substitution, scaffold stereochemistry, and the 1,3-dithianyl ring. Arrows indicate single structural changes, whereas associated LD_{50} values can be found beneath each molecule.

(Scheme 2) were found to be notably more potent than the analogous free alcohols (**12** and **14**, respectively), while the bromobenzyl carbamates **17** and **18** (Table 1, entries 10 and 11) were also active. Sulfonamide derivatives **19** and **20** (Table 1, entries 12 and 13) on the other hand had no observable effect on CLL cells.

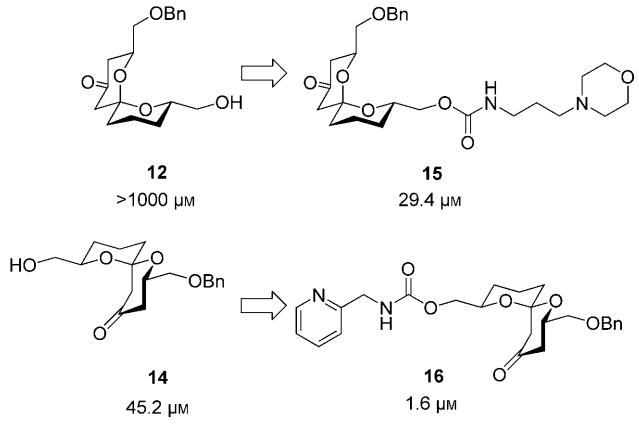

Scheme 2. Suggested spiroketal SAR: carbamate derivatisation.

appeared to be significant (Scheme 1), especially in the case of isomers **10** and **11**,[24] where the corresponding ketones **13** and **14** were measurably less potent. Carbamates **15** and **16**

For the fused bicyclic acetal series (Table 1, entries 16–26, **23**–**33**), the most potent compound in the preliminary screen was found to be **29** (LD_{50} = 0.8 μM ±0.5). Derivatising these molecules as carbamates brought a significant variation in

potency (Scheme 3). For example, the picolylcarbamate derivative bearing a 2,8-dioxabicyclo[3.2.1]octane isomeric core scaffold (**25**) was inactive, whereas its morpolinocarbamate analogue **27** induced apoptosis with an LD_{50} value of 3.4 μM (± 0.6). A comparison of these same side chains on the 6,8-dioxabicyclo[3.2.1]octane isomeric scaffold revealed the same pattern (compare **31**–**33**).

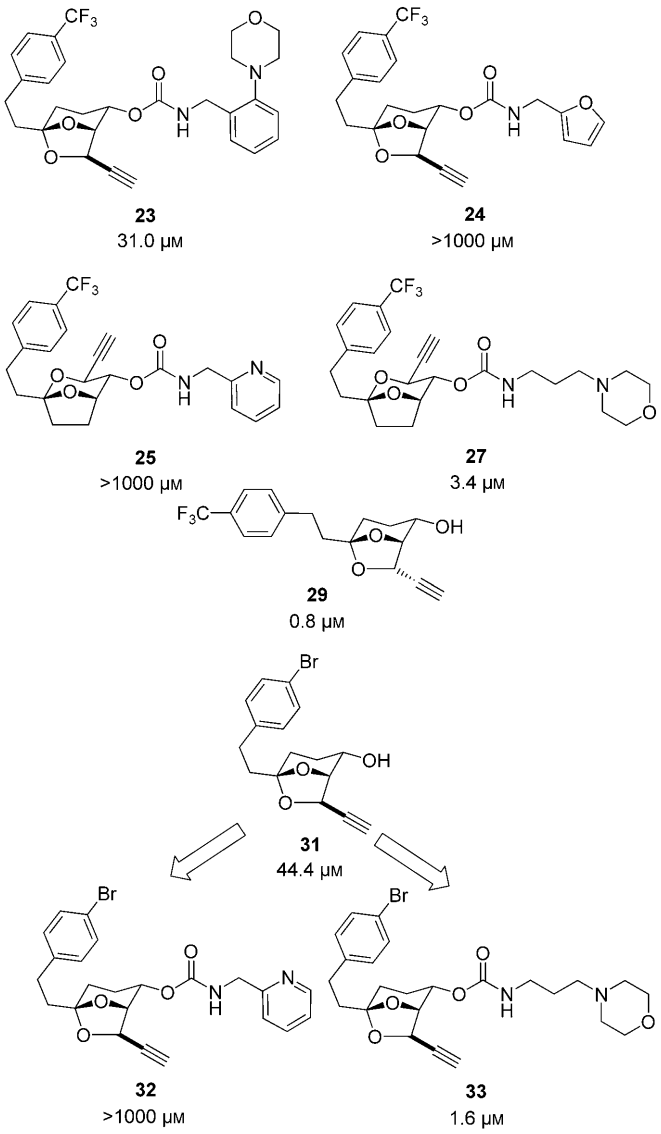

Scheme 3. Suggested fused bicyclic acetal SAR: carbamate derivatisation. Arrows indicate single structural changes, whereas associated LD_{50} values can be found beneath each molecule.

Design and synthesis of the second generation of focused libraries.

To validate the results from the first generation screen and to probe the SAR trends, a focused second generation library of spiroketal and fused bicyclic acetals were synthesised and tested.

For the spiroketals, compounds that combine the appendage groups previously highlighted as being relevant for activity were most notably targeted for synthesis (shown). Furthermore, the importance of scaffold configuration was addressed by preparing derivatives corresponding to each of the three spiroketal isomers (**34a–b, 35a–b, 36–38**, and **39a–b**) using the chemistry previously described.[17]

For the fused bicyclic acetals, a biological investigation of compounds **7** and **41**–**44** (shown) was designed to evaluate the significance of the acetylene functionality, especially in terms of the stereochemical configuration at the C3 position. Systematic variations (**45**) of the aromatic (R^2) and carbamate (R^3) residues were also explored.

For the preparation of spiroketal scaffolds **9**–**11** (Scheme 4), a modification was made to our previously published route.[17] Reaction of the lithium anion of **46** with Weinreb amide **47** formed the key intermediate **48** in excellent yield and rendered the route more amenable to large scale synthesis. For the preparation of the targeted carbamates (Scheme 4, conditions b–d, and Table 2), starting from **8**–**11** and **49**, an issue arose concerning their purification. Silica gel column chromatography facilitated the removal of the *p*-nitrophenol side product, but it also caused epimerisation at C6 in the case of the least stable spiroketal isomers—those derived from **10** and **11** (Table 1).

By stirring the crude carbamates in a dichloromethane suspension of polymer supported 1,5,7-triazabicyclo[4.4.0]dec-5-ene (TBD) for 20 min at room temperature, the *p*-nitrophenol could be effectively scavenged to leave only a short purification through florisil to deliver the pure carbamate derivatives (Table 2).

The targeted fused bicyclic acetals were prepared in a manner consistent with our previously disclosed synthesis of analogous structures (Scheme 5).[18] Butane-2,3-diacetal (BDA)-derived alcohol intermediates **53** and **54a–b** were elaborated, therefore, into their respective target molecules – **43**, **55**, and **29** – by sequential Swern oxidation, Horner–Wadsworth–Emmons olefination, enone reduction, and acid catalysed internal ketalisation steps.

These compounds were then converted to the desired carbamates using standard *N*,*N*′-disuccimidylcarbonate (DSC)-mediated coupling conditions and subsequent treatment with the requisite 2-picolyl or 3-morpholinopropyl amine (**41**–**42**, **44**, and **56**; Scheme 5).

Biological evaluation of the second generation of focused libraries

Twenty six bicyclic acetals, fifteen spiroketals (Table 3, entries 1–15) and eleven fused bicyclic acetals (Table 3, entries 16–26) including a repeat evaluation of three of the most potent compounds from the first generation screen (Table 3, entries 6, 16, and 25), were tested against primary CLL cells. The second generation compounds showed an increase in activity compared with the first generation, with LD_{50} values ranging from 0.32 to 84.3 μM, including five with submicromolar potencies.

The three repeated compounds gave reproducible activities. For the spiroketals, an additional SAR feature was identified between compounds **9**, **12**, **15**, **34a**, **35a**, and **40** (Scheme 6).

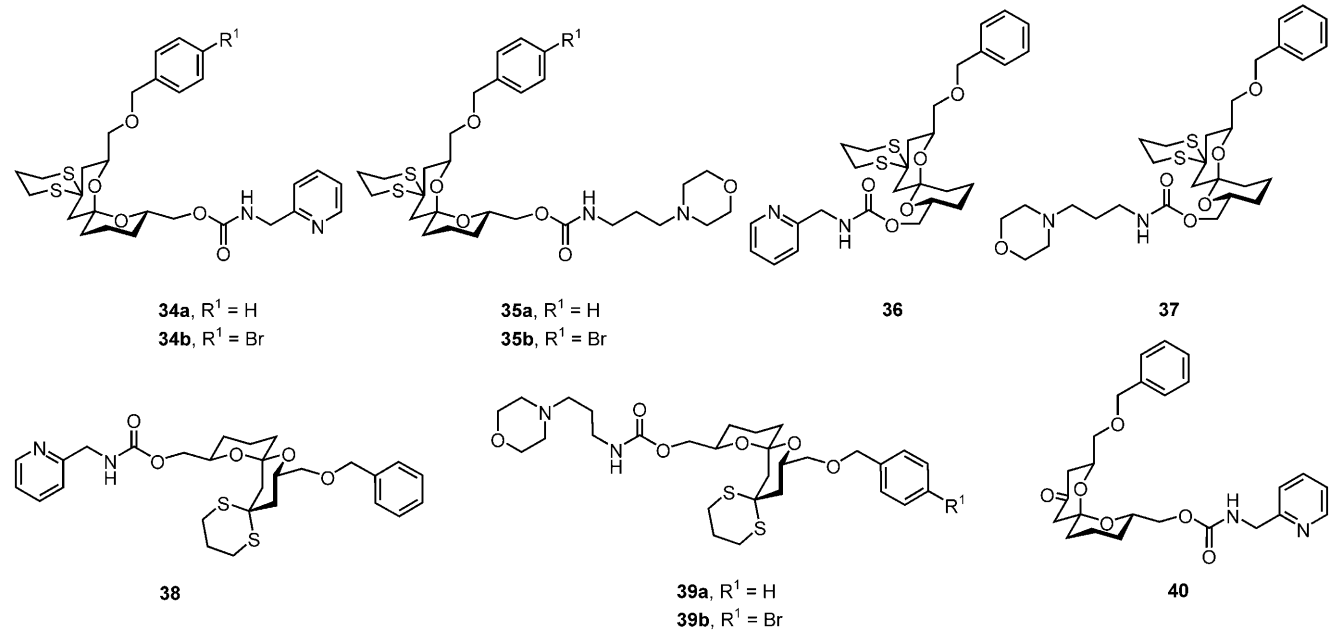

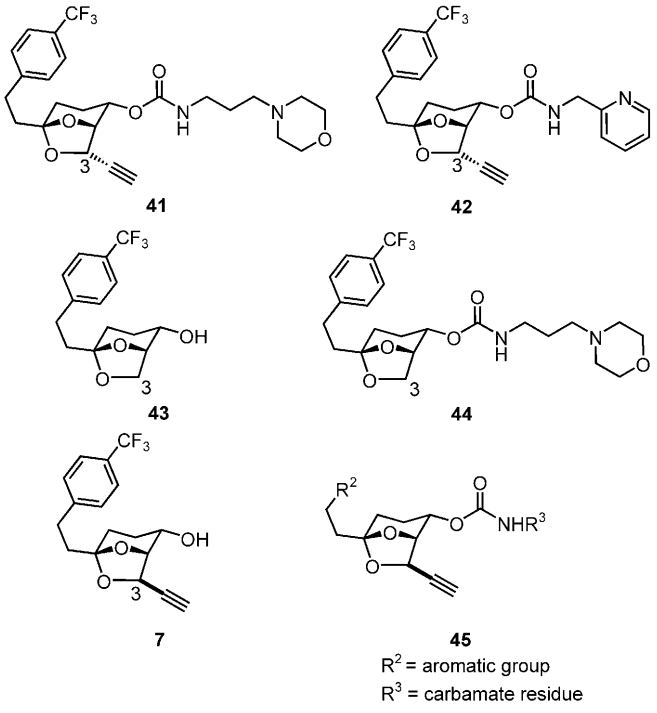

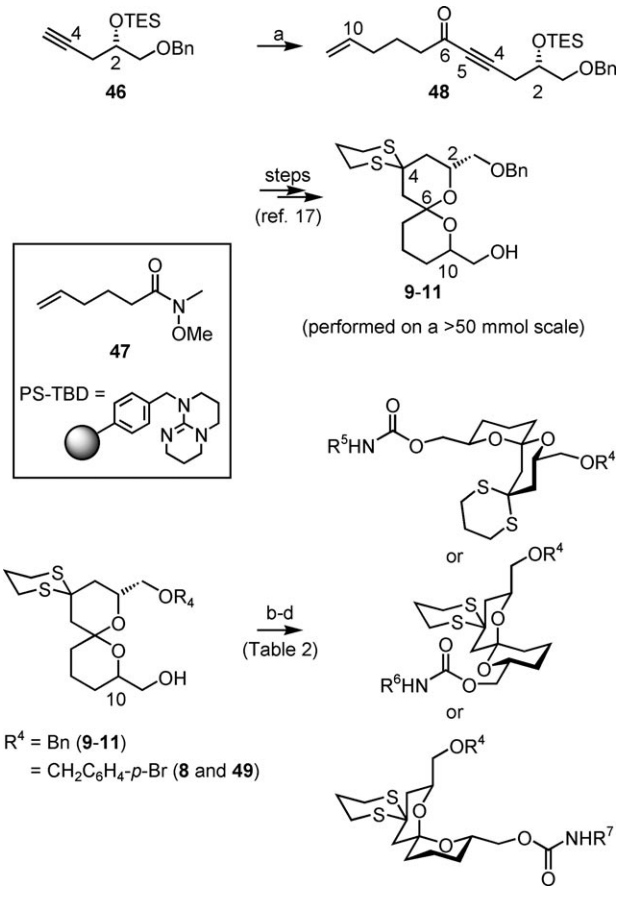

In this case, the carbamate and 1,3-dithianyl functionalities appear to act additively in terms of potency, leading to the most active spiroketal derivatives, **34a** and **35a**.

It is also important to note that differences in the absolute stereochemistry of the spiroketal structure led to measurable changes in potency (for example, compare **35a**, **37**, and **39a**; Table 3; entries 1, 7, and 13, respectively). Instead, despite the promising preliminary SAR trends in the first generation screen, derivatives bearing *p*-bromobenzyl functionality (**34b**,

Scheme 4. Synthesis of targeted spiroketal carbamates: *Reagents and conditions*: a) *i*PrMgCl (1.2 equiv), THF, −10 °C, 2 h 30 min, then **47**, THF, −40 °C to RT, 16 h, 90%, b) *p*-nitrophenylchloroformate, py, THF, RT, 20 min, c) amine, DMF, RT, 20 min, d) PS-TBD, CH_2Cl_2, RT, 2 h, 13% - quantitative, over three steps (please refer to Supporting Information). TBD = 1,5,7-Triazabicyclo[4.4.0]dec-5- ene.

35b, **39b**, and **49**) did not yield the most active compounds (Table 3; entries 4, 2, 14, and 15, respectively).

For the fused bicyclic acetals, the acetylene functionality was found to be important for activity (Scheme 7): analogue **43**, with no acetylene group present was tenfold less active than both diastereomers containing this functionality (**7** and **29**), which were interestingly equipotent. In comparison to compound **33** (Table 3, entry 25), no significant difference in potency could be found when changing the aromatic group type (Table 3, entry 24) or by varying the aromatic *p*-substituent (Table 3, entries 22 and 23). The carbamates were equally or less potent than compounds **7** and **29** from the preliminary screen. In particular, the derivatisation of compound **29** (Scheme 7) gave mixed results. Whereas the morpholinopropyl analogue **41** was over ten times less active, the 2-picolyl analogue **42** displayed comparable potency with **29** (LD_{50} = 0.63 μM ±0.3).

Studies for activity validation

To validate the active compounds prior to mode of action studies, both enantiomers of the most potent bicyclic acetals were concurrently tested against primary CLL cells. For the spiroketals, scaffold *ent*-**9** (Scheme 8) was prepared starting from (*S*)-glycidol, via alkyne *ent*-**46**. Carbamates *ent*-**34a** and *ent*-**35a** were then synthesised according to our previously established method (see Scheme 4).

Given the significant differences in potency between spiroketal carbamates **34a** and **40** (Table 3), we viewed further variation at the C4 position with significance. In this regard, spiroketal carbamates **58** and **59** (Scheme 9) were considered important targets and could be prepared in an efficient manner starting from ynone **48**. Sharpless asymmetric dihydroxylation of the terminal olefin of **48** afforded diol **60** according to the previously described procedure.[17] Lindlar reduction of **60** then led to cyclic hemiacetal **61** in good yield, which formed the unsaturated spiroketal **62** as the major spiroketal product on treatment with acid. This was then elaborated into the target carbamate **58** (Scheme 9) in a 59% yield over the two steps. Alternatively, palladium-catalysed hydrogenation of **60** led to fully-reduced ketodiol **63** in good yield (Scheme 9), which on cyclisation (**64**) and further treatment with standard carbamate forming conditions, afforded **59** in a 75% yield over the two steps. For the synthesis of *ent*-**7**, a scalable and efficient route was followed (Scheme 10), based on the recently reported synthesis of insect pheromone (1*S*,2*R*,5*R*,7*S*)-2-hydroxy-*exo*-brevicomin by Gautam et al.[25] Treatment of the crude aldehyde **66** readily prepared from cheap sugar derivative **65**[25] with phosphonate diester **57a** (Scheme 10) under modified Horner–Wadsworth–Emmons conditions afforded the *E*-enone **67** as a single diastereomer in a 48% yield over three steps. Flow hydrogenation[26] of **67** by H-Cube™ then afforded the ketone-hemiacetal mixture (**68** and **69**), which was immediately treated with TFA/H_2O to affect a trans-ketalisation to the unstable aldehyde **70**. In keeping with the overall efficiency of Gautam's synthesis, **70** could then be treated in its crude form with the Ohira–Bestmann reagent (**71**) to deliver the target molecule, *ent*-**7**, in a reasonable 41% yield over two steps. Overall, *ent*-**7**

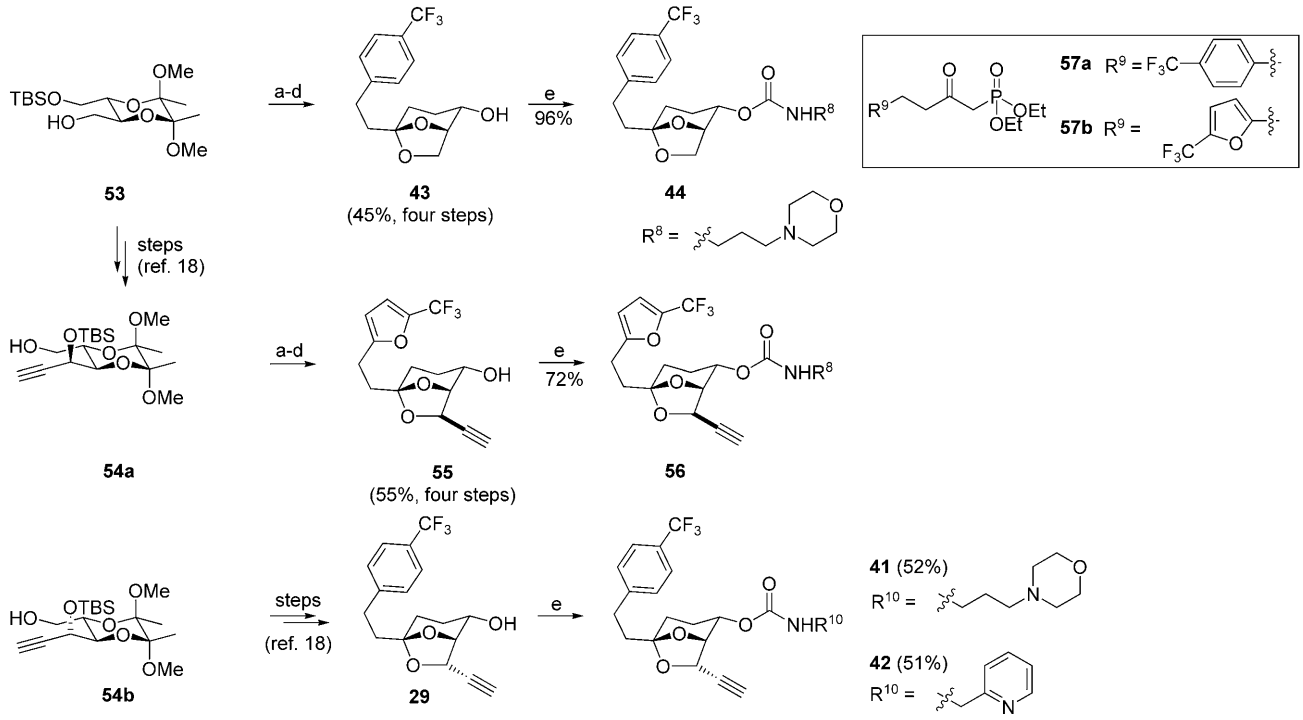

Scheme 5. Synthesis of targeted fused bicyclic acetal carbamates: *Reagents and conditions*: a) $(COCl)_2$, DMSO, CH_2Cl_2, −78 °C then Et_3N, −78 °C to RT, 1 h; b) **57a** or **57b**, LiCl, *i*Pr_2NEt, MeCN, RT, 1 h; c) $Na_2S_2O_4$, $NaHCO_3$, dioxane/H_2O, 50 °C, 5 h or H-Cube™ hydrogenation reactor, EtOH; d) 3N HCl, EtOH, 50 °C, 18 h; e) 1) DSC, MeCN, NEt_3, RT, 1 h, 2) amine, RT, 30 min. DSC=*N*,*N*′-disuccimidylcarbonate.

Table 2. Spiroketal carbamates: structures and associated yields.[a]

No.	R^4	R^5	R^6	R^7	Yield/%
38	Bn	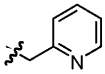	-	-	95
39a	Bn	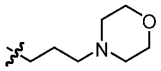	-	-	85
50	Bn	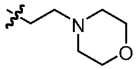	-	-	77
51	Bn	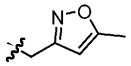	-	-	68
52	Bn	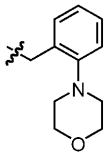	-	-	13
39b	$CH_2C_6H_4$-*p*-Br	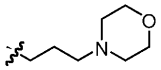	-	-	quant.
36	Bn	-	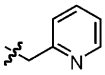	-	70
37	Bn	-	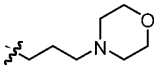	-	95
34a	Bn	-	-	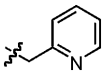	75
35a	Bn	-	-	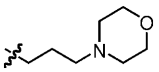	77
34b	$CH_2C_6H_4$-*p*-Br	-	-	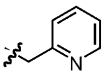	91
35b	$CH_2C_6H_4$-*p*-Br	-	-	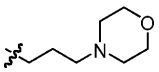	66

[a] See Scheme 4.

was prepared in a 19% yield over six steps starting from a cheap commercially available starting material with need for only two separate purification steps. The respective spectroscopic data of **7** and *ent*-**7** were identical. Chiral supercritical fluid chromatography (SFC) analysis of a 1:1 mixture and of the two pure components, combined with optical rotation measurements confirmed that the two compounds were indeed enantiomeric and with *ee* > 99% (Scheme 10).

Eight bicyclic acetals were tested against primary CLL cells, one set of fused bicyclic acetal enantiomers (Table 4, entries 1 and 2), two sets of spiroketal enantiomers (Table 4, entries 3–6), and two further spiroketal analogues (Table 4, entries 7 and 8). Those activities measured for the compounds tested in previous screens (**7**, **34a**, and **35a**) were found to be reproducible and within experimental error in this case.

Compounds *ent*-**7**, *ent*-**34a**, and *ent*-**35a** were found to possess activities of the same order of magnitude as their corresponding enantiomers. The significance of this result will be examined further in follow-up studies. Encouragingly, spiroketals **58** and **59** achieved similar levels of potency to **34a**.

On four selected compounds further studies were conducted to investigate the specific mechanism of cell death (Figure 2). The results clearly indicate that both sets of molecules induce CLL cell death via an apoptotic pathway, rather than by necrosis as evidenced by the concentration-dependent increase in caspase-3 activation following in vitro culture (Figure 2).

Conclusions

For each of the spiroketal and fused bicyclic acetal series of compounds, submicromolar LD_{50} values were achieved through the screening of no more than twenty-nine unique analogues.

The first generation screen led to a spectrum of activity in line with structural differences based around the bicyclic acetal core and it was possible to use SAR trends to improve the overall potency of both series in the case of a second generation of compounds. These preliminary data were then validated by reproducing the activity of the most potent compounds in subsequent screens. The most potent compounds were approximately one logarithmic unit more potent as primary CLL cytotoxic agents than fludarabine (6.2 μM (±7.5)), the most competitive single chemotherapeutic on today's market when compared like-for-like in the same cell based assay.[27] Furthermore, twenty one of the twenty-six second generation compounds (ten out of fifteen spiroketals and the entire fused bicyclic acetal set) showed equal or greater potency than fludarabine. The fact that the most potent molecules from each series (**7** and **34a**) are structurally quite different is also interesting to note. Furthermore, we showed that the compounds induce CLL cell death via an apoptotic pathway, rather than by necrosis.

Therefore, promising active compounds have been identified that we believe warrant further attention as potential anticancer agents. In this regard, biological investigations into the mode of action of these molecules are underway in our laboratories. In particular, we now want to elucidate the principal biological targets of these compounds by performing pharmacogenomic profiling (that is, gene expression profiling of primary tumour samples treated with agent using untreated

Table 3. Second generation screening results.

Entry	Structure	Cmpd no. (purity)[a]	LD_{50} [μM] (±S.D.)
1	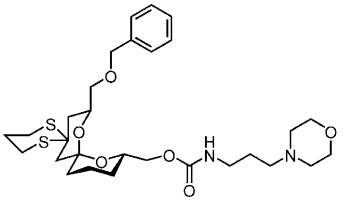	**35a** (95)	0.92 (0.2)
2	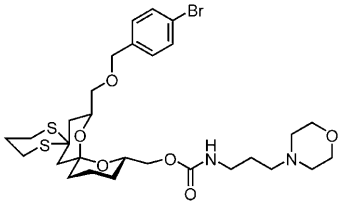	**35b** (95)	1.8 (0.2)
3	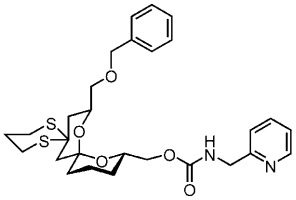	**34a** (95)	0.32 (0.4)
4	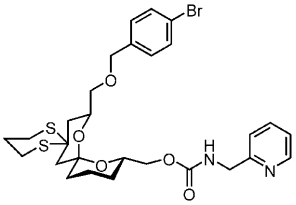	**34b** (95)	2.0 (0.4)
5	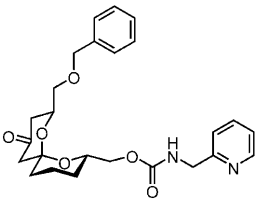	**40** (95)	21.3 (0.4)
6	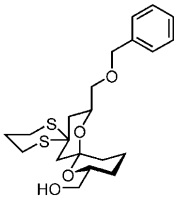	**10** (95)	1.1 (0.5)
7	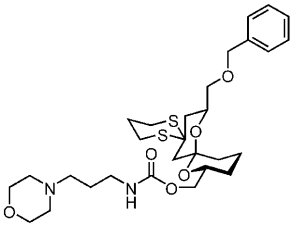	**37** (95)	4.1 (0.2)

Table 3. (Continued)

Entry	Structure	Cmpd no. (purity)[a]	LD_{50} [μM] (±S.D.)
8	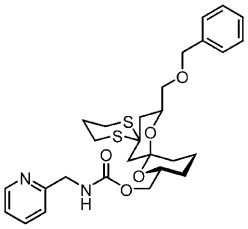	**36** (85)	1.0 (0.6)
9	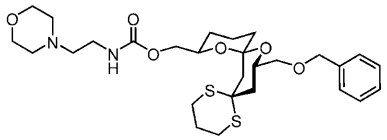	**50** (95)	45.4 (0.6)
10	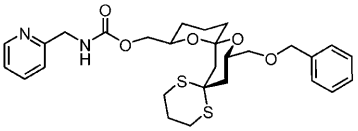	**38** (95)	2.5 (0.4)
11	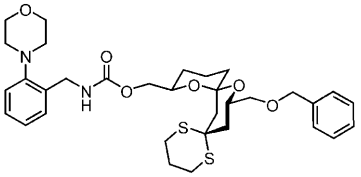	**52** (95)	84.3 (0.4)
12	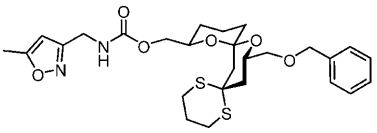	**51** (95)	32.2 (0.6)
13	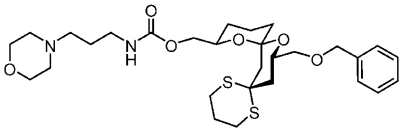	**39a** (90-95)	6.4 (0.3)
14	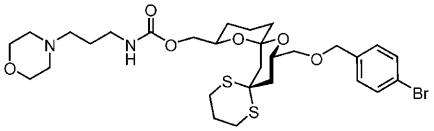	**39b** (90-95)	12.7 (0.2)
15	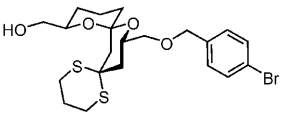	**49** (95)	1.0 (0.4)
16	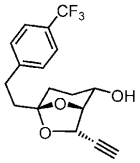	**29** (95)	0.33 (0.6)
17	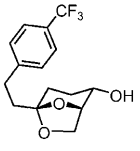	**43** (95)	2.8 (0.3)

Table 3. (Continued)

Entry	Structure	Cmpd no. (purity)[a]	LD_{50} [μM] (±S.D.)
18	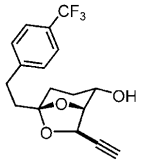	**7** (95)	0.34 (0.3)
19	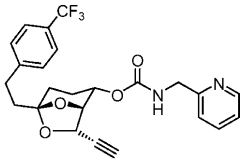	**42** (95)	0.63 (0.3)
20	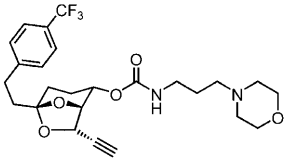	**41** (95)	5.2 (0.4)
21	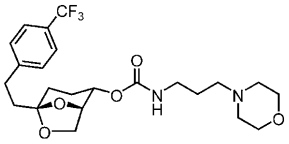	**44** (95)	2.7 (0.4)
22	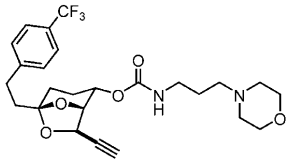	**5** (90-95)	2.1 (0.3)
23	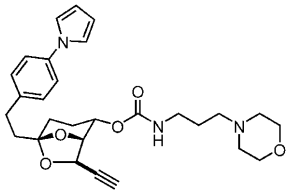	**45a**[b] (90-95)	1.9 (0.3)
24	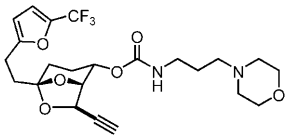	**56** (90)	3.8 (0.6)
25	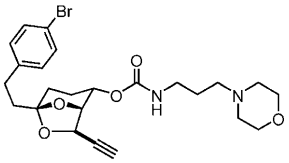	**33** (95)	2.3 (0.5)
26	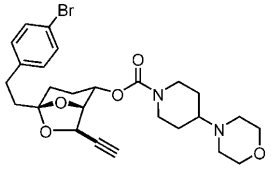	**45b** (95)	6.0 (0.6)

[a] Compound purity determined spectroscopically using ^{1}H NMR and LC-MS; [b] see the Supporting Information for the synthesis and characterisation of compound **45a**.

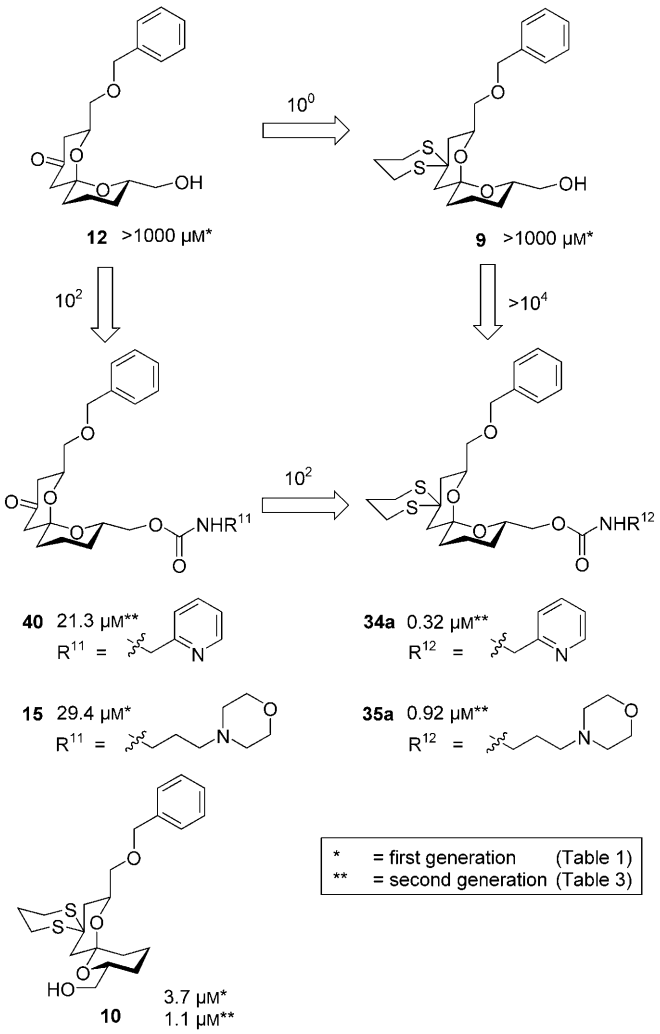

Scheme 6. Identification of the most potent spiroketal derivatives (**34a** and **35a**) and validation of compound series by repeat screening of compound **10**. Arrows indicate single structural changes, whereas associated LD_{50} values can be found beneath each molecule.

samples as comparators). In addition, we will also subject these molecules to a broad-spectrum kinase screening assay to assess their effects on kinase activity. We also plan to assess the relative cytotoxicity of these agents in normal tissue and tumour cells in an effort to establish whether they possess a positive therapeutic index that could be exploited clinically in the future. The inactivity of **7** towards MCF7 and A549 cell proliferation, for example, provides a positive first indication of selectivity.[18]

Experimental Section

Chemistry

General procedure for spiroketal carbamate formation using polymer supported 1,5,7-Triazabicyclo[4.4.0]dec-5-ene (TBD): Pyridine (2.5 equiv) and *p*-nitrophenylchloroformate (2.5 equiv) was added sequentially, in one portion, at 0 °C to a THF solution (0.15 M) of the spiroketal alcohol. The reaction was then left to stir at RT for 30 min, then Et_2O and distilled water were added, and the subsequent aqueous

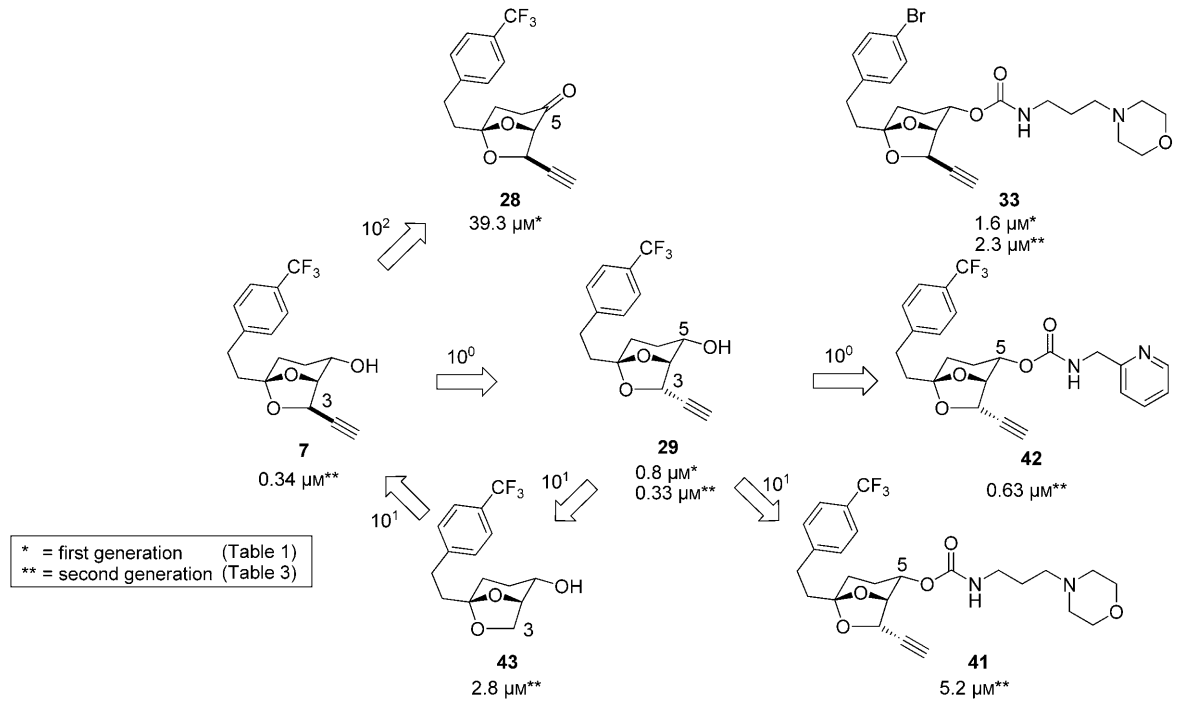

Scheme 7. Identification of the most potent fused bicyclic acetal derivatives, validation of compound series by repeat screening of compounds **29** and **33**, and derivatisation of compound **29**. Arrows indicate single structural changes, whereas associated LD_{50} values can be found beneath each molecule.

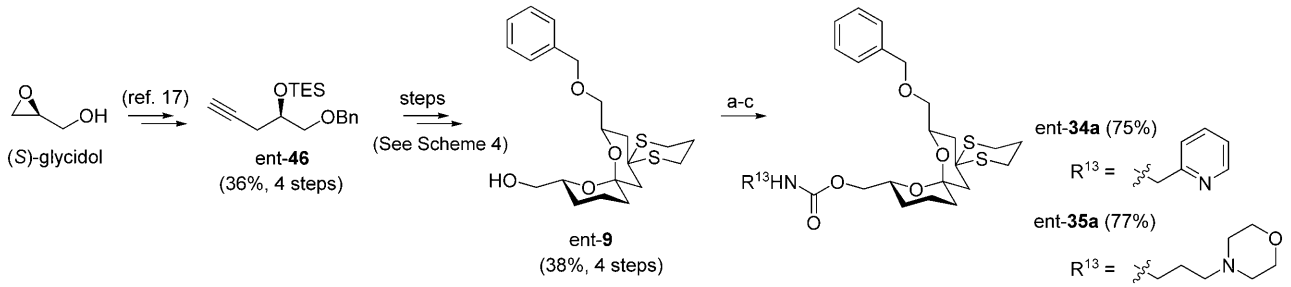

Scheme 8. Synthesis of spiroketal carbamates *ent*-**34a** and *ent*-**35a**: *Reagents and conditions*: a) *p*-nitrophenylchloroformate, py, THF, RT, 30 min; b) amine, DMF, RT, 15 min; c) PS-TBD, CH_2Cl_2, RT, 2 h.

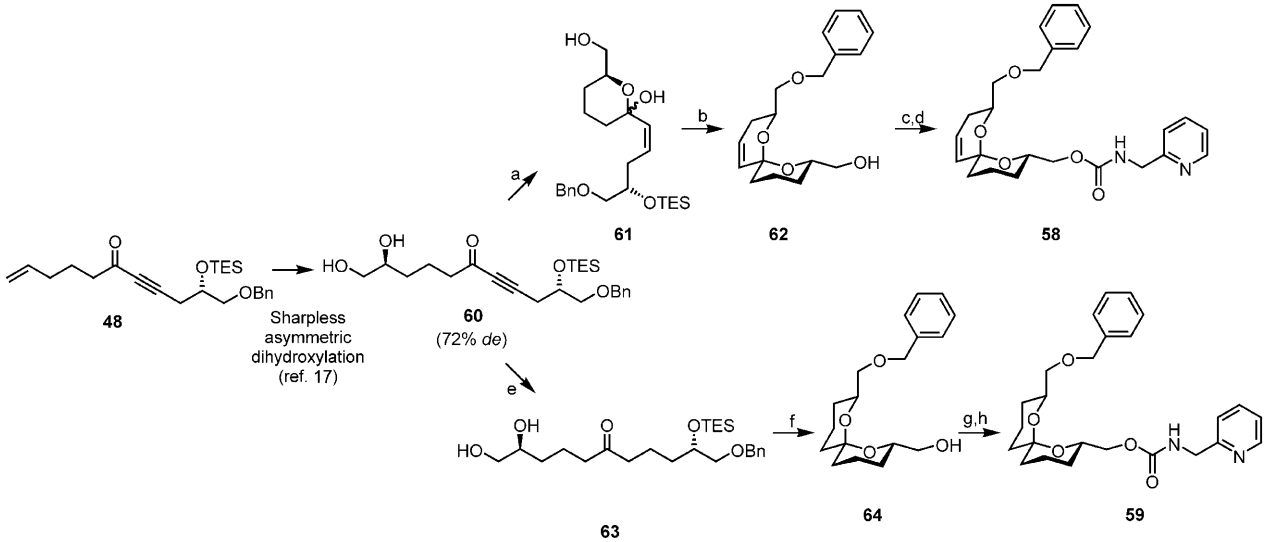

Scheme 9. Synthesis of spiroketals **58** and **59**: *Reagents and conditions*: a) 5% Pd/$CaCO_3$, $Pb(OAc)_2$, quinoline (1 equiv), MeOH or PhMe, H_2, 30 min, RT, 77%; b) $HClO_4$ 10% aq., MeCN/CH_2Cl_2, 1 h, 0 °C, 75%; c) *p*-nitrophenylchloroformate, py, THF, RT, 30 min; d) 2-picolylamine, DMF, RT, 15 min, 78%; e) 10% Pd/C or 5% Pd/$CaCO_3$, $Pb(OAc)_2$, PhMe, H_2, 30 min, RT, 75%; f) $HClO_4$ 10% aq., MeCN/CH_2Cl_2, 1 h, 0 °C, 88%; g) *p*-nitrophenylchloroformate, py, THF, RT, 30 min; h) 2-picolylamine, DMF, RT, 15 min, 85%.

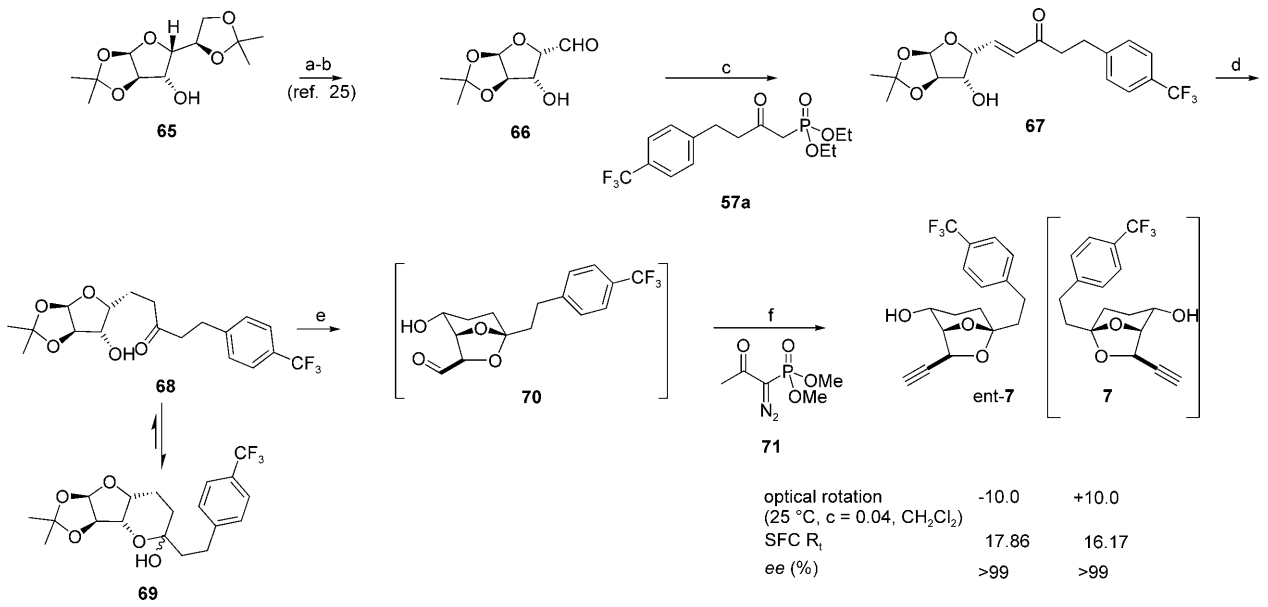

Scheme 10. Synthesis of fused bicyclic acetal *ent*-**7**: *Reagents and conditions*: a) aq. AcOH, RT, 12 h; b) aq. $NaIO_4$, MeOH, RT, 1 h; c) **57a**, LiCl, *i*Pr_2NEt, MeCN, RT, 1 h, 48%, over 3 steps; d) H_2, H-cube™ hydrogenation reactor, 10% Pd/C, THF, RT, 2 h, 96%; e) TFA/H_2O, 0 °C to RT, 16 h; f) **71**, K_2CO_3, MeOH, RT, 5 h, 41%, two steps.

Table 4. Enantiomer and further analogue screening results.

Entry	Structure	Cmpd no. (purity)	LD_{50} [μM] (±S.D.)
1	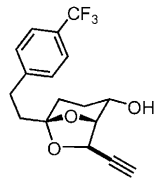	**7** (>95)[a]	0.22 (0.3)
2	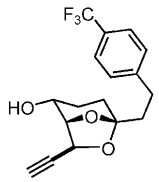	*ent*-**7** (>95)[a]	0.50 (0.2)
3	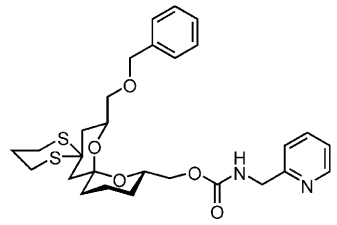	**34a** (>95)[b]	0.17 (0.3)
4	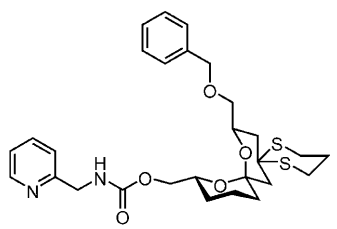	*ent*-**34a** (95)[b]	0.86 (0.2)
5	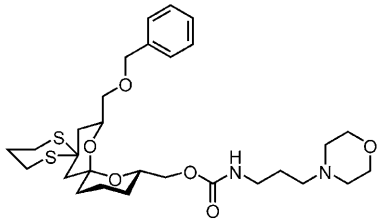	**35a** (>95)[b]	0.92 (0.4)
6	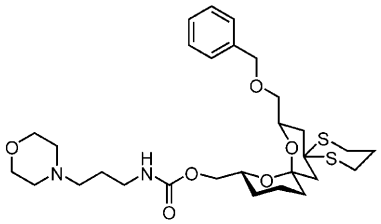	*ent*-**35a** (>95)[b]	1.1 (0.5)
7	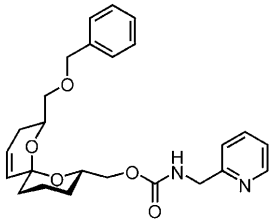	**58** (>95)[b]	0.27 (0.5)
8	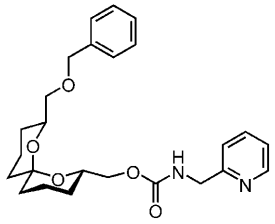	**59** (>95)[b]	0.67 (0.6)

[a] Compound purity determined by elemental analysis; [b] compound purity determined spectroscopically using ^{1}H NMR and LC-MS.

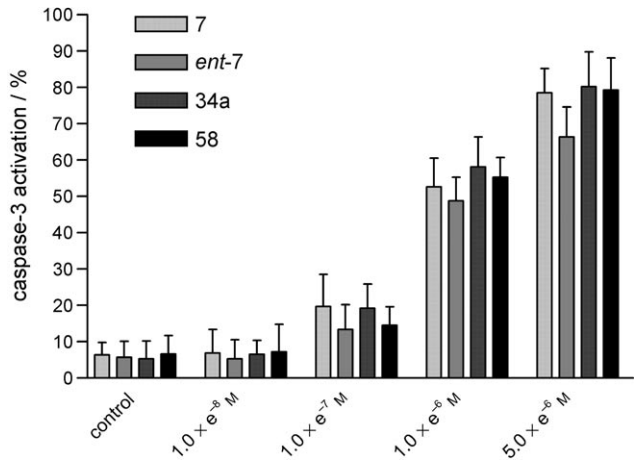

Figure 2. Concentration-dependent increase in caspase-3 activation following exposure of primary CLL cells to compounds **7**, *ent*-**7**, **34a**, and **58**. Experiments were all carried out in triplicate and results expressed as mean values ± SEM.

phase extracted with Et_2O (×3). The combined organic extracts were washed with distilled water (×1) and brine (×1), dried, filtered, and then evaporated in vacuo. The crude was then redissolved in DMF (0.15 M) and treated with the amine (2.0 equiv), dropwise. After stirring for 20 min, EtOAc and distilled water were added, and the subsequent aqueous phase extracted with EtOAc (×4). The combined organic extracts were washed with distilled water (×1) and brine (×1), dried, filtered, and then evaporated in vacuo to afford a crude oil. Scavenging of *p*-nitrophenol was performed by dissolving the crude in DCM (0.005 M), adding polymer supported TBD (2.7 equiv) to the solution, and stirring gently for 2 h. The mixture was then filtered and evaporated in vacuo. The resultant crude was purified by gravimetric column chromatography on florisil using EtOAc as eluent to afford the carbamate. Please see Supporting Information for analytical data for all carbamate derivatives.

Fused Bicyclic Acetal ent-7: The phosphonate ester **57a** (150 mg, 0.42 mmol) and anhydrous LiCl (36 mg, 0.85 mmol) were added to a stirred suspension of the crude aldehyde **66** (80 mg, 0.43 mmol assumed pure) in 2 mL of $MeCN/CH_2Cl_2$ (11:5). Then iPr_2NEt (75 μL, 0.42 mmol) was added dropwise. The resultant solution was vigorously stirred for 1 h 30 min. The reaction mixture was then evaporated in vacuo to afford the crude enone, which was subsequently purified by column chromatography on silica gel using EtOAc and petroleum ether as eluent (90 mg, 0.21 mmol) to provide pure **67** as a white solid (48% assuming the crude aldehyde to be pure); A 100 mL flask containing a solution of **67** (0.71 g, 1.84 mmol) in THF (40 mL) was then placed at a designated position and introduced into the H-Cube™ flow hydrogenation reactor equipped with a 10% Pd/C cartridge using loop injection. The system automatically stabilised at 60 °C and 0.6 mL min^{-1} flow rate. The product was collected as a white solid after removal of the solvent in vacuo (0.75 g of which 10% of the weight was THF according to ^1H NMR, 1.76 mmol, 96%). The ketone/hemiacetal mixture (**68**/**69**, 239 mg, 0.615 mmol) was then added to a solution of TFA/distilled H_2O cooled to 0 °C (3 mL, 3:2) and the mixture was stirred for 2 h at 0 °C and then 11 h at RT. The solvent was evaporated and the resultant crude aldehyde (**70**) taken up in MeOH (17 mL). Ohira–Bestmann reagent (**71**, 156 mg, 0.812 mmol) and anhydrous K_2CO_3 (187 mg, 1.35 mmol) were then added at RT under vigorous stirring. After 5 h the mixture was diluted with EtOAc and neutralised using a saturated aqueous solution of NH_4Cl. Distilled H_2O was added and the aqueous phase extracted with EtOAc (×2), and the recombinant organic extracts were washed with brine (×1). Drying, filtration, and evaporation of the organic solvents in vacuo yielded a crude oil, which was purified by gravimetric column chromatography on silica using petroleum ether and Et_2O as eluent (from 7:3 to 3:7) to afford *ent*-**7** as a white solid (82 mg, 41% over two steps): R_f 0.31 (7:3 Et_2O:petroleum ether); m.p. 56–57 °C; $[\alpha]_D$ −10.0 (c 0.04, CH_2Cl_2); δ_H ($CDCl_3$, 600 MHz) 7.53 (2H, d, J=8.0, *Ar*, H_{10-III} and H_{10-V}), 7.34 (2H, d, J=8.0, *Ar*, H_{10-II} and H_{10-VI}), 4.96 (1H, d, J=1.6, H_3), 4.43 (1H, broad d, J=3.5, H_4), 3.97–4.02 (1H, m, H_5), 2.85–2.96 (2H, m, H_{10}), 2.47 (1H, d, J=2.1, H_1), 2.03–2.07 (2H, m, H_9), 1.95–1.99 (1H, m, H_{6A}), 1.60–1.77 (4H, m, H_{6B}, H_7 and -O*H*); δ_C ($CDCl_3$, 150 MHz) 146.4 (*Ar*, C_{10-I}), 128.8 (*Ar*, C_{10-II} and C_{10-VI}), 128.1 (quartet, J^{C-F}=31.6, *Ar*, C_{10-IV}), 125.2 (quartet, J^{C-F}=3.0, *Ar*, C_{10-III} and C_{10-V}), 124.3 (quartet, J^{C-F}=270.3, -*C*F_3), 109.6 (C_8), 83.3 (C_4), 82.7 (C_2), 72.8 (C_1), 65.9 (C_3 and C_5), 37.4 (C_9), 33.8 (C_7), 28.8 (C_{10}) and 26.2 (C_6); ν_{max} (film)/cm^{-1} 3311 (broad m, -OH and terminal acetylene) and 2954 (m, C-H); LC/MS ($MeCN/H_2O$ 1:1): R_t=3.65 (+ES MS: 327.2 (MH^+), single component); *m/z* (+ESI) calc. for $C_{17}H_{17}F_3O_3Na$ (MNa^+) 349.1027, found 349.1044; Chiral SFC (9:1 hexanes:*i*PrOH): pre-prepared 1:1 mixture of **7** and *ent*-**7**: 16.2 min (**7**), 17.9 min (*ent*-**7**); pure *ent*-**7**: 17.9 min; >99% ee; Elemental analysis (%): Calc. C, 62.57; H, 5.25; Found. C, 62.54; H, 5.39. Please see the Supporting Information for the full compound numbering for *ent*-**7**.

Full experimental and analytical data for all other new compounds can be found in the Supporting Information.

Biological Studies

Primary CLL cell culture conditions: Peripheral blood samples from the CLL patients used in this study were obtained with the patients' informed consent. All studies were conducted in accordance with the ethical approval granted by the South East Wales Research Ethics Committee (02/4806). Freshly isolated peripheral blood CLL cells (1×10^6 mL^{-1}) were cultured in RPMI medium (Invitrogen, Paisley, UK) supplemented with 100 units mL^{-1} penicillin, 100 μg mL^{-1} streptomycin and 10% foetal calf serum. Cells were incubated at 37 °C in a humidified 5% CO_2 atmosphere in the presence of each compound (10^{-9}-5×10^{-6} M). All compounds were made up in DMSO and were evaluated in serial dilutions against primary CLL cells. In addition, control cultures were carried out to which no drug was added. The cytotoxic effects of the compounds were quantified using an Annexin V/propidium iodide flow cytometry assay (Bender Medsystems, Vienna, Austria). All assays were performed in duplicate and LD_{50} values were calculated from sigmoidal dose-response curves using Prism 3.0 software (Graphpad Software Inc., San Diego, CA). The sigmoidal dose-response curves were derived by plotting log[compound concentration] against the percentage apoptosis induced by that concentration. A wide range of concentrations were used to establish the biologically active range for each individual compound.

Caspase-3 activation assay: CLL cells were incubated at 37 °C in a humidified 5% CO_2 atmosphere in the presence of compounds **7**, *ent*-**7**, **34a**, and **58** (10^{-7}-5×10^{-6} M). Cells were then harvested by centrifugation and were incubated for 1 h at 37 °C in the presence of the PhiPhiLux™ G_1D_2 substrate (Calbiochem, Nottingham, UK). The substrate contains two fluorophores separated by a quenching linker sequence that is cleaved by active caspase-3. Once cleaved,

the resulting products fluoresce green and can be quantified using flow cytometry.

Acknowledgements

The authors thank Pfizer Global Research and Development, Sandwich, UK for funding (S.V.L.), the EPSRC for a studentship (L.-G.M.), the Swiss National Science Foundation for a research fellowship (F.L.) the Marie Curie Fellowship for a research fellowship (G.Z.), the Cambridge Overseas Trust (Z.Q.) and Leukaemia Research UK (C.P. and C.F.) for funding. The authors also thank Dr. Deborah Longbottom for her helpful assistance with the preparation of this manuscript.

Keywords: structure–activity relationships · natural products · drug design · apoptosis · leukaemia

[1] R. L. Auer, J. Gribben, F. E. Cotter, *Br. J. Haematol.* **2007**, *139*, 635.
[2] J. C. Byrd, S. Stilgenbauer, I. W. Flinn, *Hematology* **2004**, *1*, 163.
[3] T. Robak, M. Kasznicki, *Leukemia* **2002**, *16*, 1015.
[4] M. J. Keating, S. O'Brien, S. Lerner, C. Koller, M. Beran, L. E. Robertson, E. J. Freireich, E. Estey, H. Kantarjian, *Blood* **1998**, *92*, 1165.
[5] V. A. Morrison, K. R. Rai, B. L. Peterson, J. E. Kolitz, L. Elias, F. R. Appelbaum, J. D. Hines, L. Shepherd, R. E. Martell, R. A. Larson, C. A. Schiffer, *J. Clin. Oncol.* **2001**, *19*, 3611.
[6] P. Hillmen, A. Skotnicki, T. Robak, B. Jaksic, A. Dmoszynska, C. Sirard, J. Mayer, *J. Clin. Oncol.* **2006**, *24*, 6511.
[7] L. Alinari, R. Lapalombella, L. Andritsos, R. A. Baiocchi, T. S. Lin, J. C. Byrd, *Oncogene* **2007**, *26*, 3644.
[8] S. Demko, J. Summers, P. Keegan, R. Pazdur, *Oncologist* **2008**, *13*, 167.
[9] D. Catovsky, S. Richards, E. Matutes, D. Oscier, M. J. S. Dyer, R. F. Bezares, A. R. Pettitt, T. Hamblin, D. W. Milligan, J. A. Child, M. S. Hamilton, C. E. Dearden, A. G. Smith, A. G. Bosanquet, Z. Davis, V. Brito-Babapulle, M. Else, R. Wade, P. Hillmen, *Lancet* **2007**, *370*, 230.
[10] B. F. Eichhorst, R. Busch, G. Hopfinger, R. Pasold, M. Hensel, C. Steinbrecher, S. Siehl, U. Jager, M. Bergmann, S. Stilgenbauer, C. Schweighofer, C. M. Wendtner, H. Dohner, G. Brittinger, B. Emmerich, M. Hallek, *Blood* **2006**, *107*, 885.
[11] F. Bosch, A. Ferrer, N. Villamor, M. Gonzalez, J. Briones, E. Gonzalez-Barca, E. Abella, S. Gardella, L. Escoda, E. Perez-Ceballos, A. Asensi, M. J. Sayas, L. Font, A. Altes, A. Muntanola, P. Bertazzoni, M. Rozman, M. Aymerich, E. Gine, E. Montserrat, *Clin. Cancer Res.* **2008**, *14*, 155.
[12] T. Robak, *Cancer Treat. Rev.* **2007**, *33*, 710.
[13] G. Del Poeta, *Cancer* **2008**, *112*, 119.
[14] C. Pepper, H. Lowe, C. Fegan, C. Thurieau, D. E. Thurston, J. A. Hartley, P. Delavault, *Br. J. Cancer* **2007**, *97*, 253; C. Pepper, R. M. Hambly, C. D. Fegan, P. Delavault, D. E. Thurston, *Cancer Res.* **2004**, *64*, 6750.
[15] K. Kojima, M. Konopleva, T. McQueen, S. O'Brien, W. Plunkett, M. Andreeff, *Blood* **2006**, *108*, 993.
[16] a) P. Dreger, E. Montserrat, *Leukemia* **2002**, *16*, 985; b) J. C. Byrd, S. Stilgenbauer, I. W. Flinn, *Hematology* **2004**, *1*, 163.
[17] G. Zinzalla, L.-G. Milroy, S. V. Ley, *Org. Biomol. Chem.* **2006**, *4*, 1977.
[18] L.-G. Milroy, G. Zinzalla, G. Prencipe, P. Michel, S. V. Ley, M. Gunaratnam, M. Beltran, S. Neidle, *Angew. Chem.* **2007**, *119*, 2545; *Angew. Chem. Int. Ed.* **2007**, *46*, 2493.
[19] For an excellent review of spiroketal containing natural products, see: F. Perron, K. F. Albizati, *Chem. Rev.* **1989**, *89*, 1617; For a review of spiroketal and fused bicyclic acetal containing natural products, see: H. Kiyota, *Marine Natural Products*, Springer, Berlin **2006**, p. 65 (Topics in Heterocyclic Chemistry, No. 5).
[20] M. Ball, M. J. Gaunt, D. F. Hook, A. S. Jessiman, S. Kawahara, P. Orsini, A. Scolaro, A. C. Talbot, H. R. Tanner, S. Yamanoi, S. V. Ley, *Angew. Chem.* **2005**, *117*, 5569; *Angew. Chem. Int. Ed.* **2005**, *44*, 5433.
[21] S. V. Ley, A. C. Humphries, H. Eick, R. Downham, A. R. Ross, R. J. Boyce, J. B. J. Pavey, J. Pietruszka, *J. Chem. Soc. Perkin Trans. 1* **1998**, 3907.
[22] S. S. Mitchell, D. Rhodes, F. D. Bushman, D. J. Faulkner, *Org. Lett.* **2000**, *2*, 1605.
[23] In this case, the LD_{50} value is defined as the concentration at which each compound tested induced 50% cell death in the cell cultures as quantified by Annexin V positivity.
[24] We propose a structural reassignment of spiroketal **10** originally reported in reference [17] based on fresh analytical data. Please refer to the Supporting Information for further discussion.
[25] D. Gautam, D. N. Kumar, B. V. Rao, *Tetrahedron: Asymmetry* **2006**, *17*, 819.
[26] Based on previously developed unpublished Ley group methdology. For an example of continuous flow hydrogenation of unsaturated systems, please see: S. Saaby, K. R. Knudsen, M. Ladlow, S. V. Ley, *Chem. Commun.* **2005**, 2909.
[27] C. J. Pepper, A. Thomas, T. Hoy, C. Fegan, P. Bentley, *Br. J. Haematol.* **2001**, *114*, 70.

Received: August 7, 2008
Revised: August 29, 2008
Published online on November 21, 2008

